Model reduction for controller design for infinite-dimensional systems

Opmeer, Mark Robertus

Chapter 15

An example

We consider the robust stabilization of a beam. In Section 15.2 we show that the conditions under which we have convergence of LQG-balanced truncations are satisfied for this example. Section 15.3 contains numerical results for this example.

15.1 The model

The system we consider is a one-dimensional Euler-Bernoulli beam with Voigt-damping and with free ends. The measurements are the displacement and the angle of rotation of the middle of the beam. As actuators we choose a force and a moment at the middle of the beam.

We obtain the partial differential equation

$$\frac{\partial^2 w}{\partial t^2} + \beta \frac{\partial^5 w}{\partial x^4 \partial t} + \alpha \frac{\partial^4 w}{\partial x^4} = \frac{u_1 \delta - u_2 \delta'}{\rho a},$$

$$\alpha \frac{\partial^2 w}{\partial x^2}(-1,t) + \beta \frac{\partial^3 w}{\partial x^2 \partial t}(-1,t) = 0, \quad \alpha \frac{\partial^2 w}{\partial x^2}(1,t) + \beta \frac{\partial^3 w}{\partial x^2 \partial t}(1,t) = 0,$$

$$\alpha \frac{\partial^3 w}{\partial x^3}(-1,t) + \beta \frac{\partial^4 w}{\partial x^3 \partial t}(-1,t) = 0, \quad \alpha \frac{\partial^3 w}{\partial x^3}(1,t) + \beta \frac{\partial^4 w}{\partial x^3 \partial t}(1,t) = 0,$$

$$y(t) = \begin{bmatrix} w(0,t) \\ \frac{\partial w}{\partial x}(0,t) \end{bmatrix},$$

where $w(t,x)$ is the displacement of the beam at position $x \in (-1,1)$ at time t, $u_1(t)$ is the force applied and $u_2(t)$ the moment applied to the middle ($x = 0$) of the beam, $y(t)$ holds the measurements, ρ, a, α and β are (positive) physical parameters and δ is the Dirac delta distribution and δ' is its distributional derivative. A derivation of this model from physical considerations is given in Bontsema [6].

We put the above partial differential equation in an abstract operator-theoretic framework. We note that the spaces H^s used in this section are Sobolev spaces. Define the operator $L : D(L) \subset L^2(-1,1) \to L^2(-1,1)$ as

$$L := \frac{d^4}{d\xi^4},$$

$$D(L) := \left\{ w \in H^4(-1,1) : \frac{d^2w}{d\xi^2}(-1) = \frac{d^2w}{d\xi^2}(1) = \frac{d^3w}{d\xi^3}(-1) = \frac{d^3w}{d\xi^3}(1) = 0 \right\}.$$

It is elementary to show that L is a densely defined nonnegative operator. We define the spaces $\mathscr{X} := D(L^{1/2}) \times L^2(-1,1)$, $\mathscr{U} := \mathbb{C}^2$, $\mathscr{Y} = \mathbb{C}^2$ and the following operators. The operator $A : D(A) \subset \mathscr{X} \to \mathscr{X}$ is defined by

$$A \begin{bmatrix} x_1 \\ x_2 \end{bmatrix} := \begin{bmatrix} x_2 \\ -\alpha L\left(x_1 + \frac{\beta}{\alpha} x_2\right) \end{bmatrix},$$

$$D(A) := \left\{ \begin{bmatrix} x_1 \\ x_2 \end{bmatrix} \in \mathscr{X} : x_2 \in D(L^{1/2}), x_1 + \frac{\beta}{\alpha} x_2 \in D(L) \right\}.$$

The operator B is defined through its adjoint $B^* : D(A) \subset \mathscr{X} \to \mathscr{U}$

$$B^* \begin{bmatrix} x_1 \\ x_2 \end{bmatrix} := \frac{1}{\rho a} \begin{bmatrix} x_2(0) \\ x_2'(0) \end{bmatrix}.$$

The operator $C : D(A) \subset \mathscr{X} \to \mathscr{Y}$ is defined by

$$C \begin{bmatrix} x_1 \\ x_2 \end{bmatrix} := \frac{1}{\rho a} \begin{bmatrix} x_1(0) \\ x_1'(0) \end{bmatrix}.$$

The feedthrough operator D is taken equal to zero. In Bontsema [6] it is shown that this is indeed a representation of the partial differential equation obtained earlier.

15.2 Theoretical results

The next proposition shows that our beam system has a compact LQG-balanced realization and the error bound (14.5) holds.

Proposition 15.1. *The system considered satisfies all the assumptions of Proposition 14.46.*

Proof. If follows from Bontsema [6, Lemma 2.13] that the system under consideration is a well-posed linear system, which implies that it is an exponentially bounded distributional resolvent linear system. The input and output space are both two-dimensional. It remains to show that the finite cost condition and the dual finite cost condition are satisfied, and that the LQG-characteristic values form a summable sequence.

A spectral decomposition of the main operator A as performed in Bontsema [6] shows that A has α/β in its continuous spectrum, the other spectral points are eigenvalues and these are either located on a circle with center $-\alpha/\beta$ and radius α/β or on the negative part of the real line (see figure 15.1).

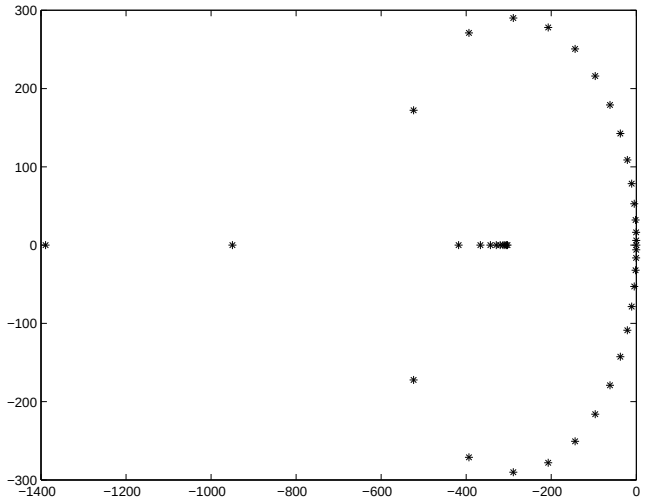

Figure 15.1: Eigenvalues of the A operator of the beam

All spectral points are in the open left half-plane, except for a quadruple eigenvalue at zero. From the above spectral decomposition one can conclude that the operator A generates an analytic semigroup (this follows as in the appendix of Chen and Triggiani [8]). It is shown in Bontsema [6] that the control operator B is unbounded, but not maximally unbounded and that the observation operator C is bounded. Using the spectral decomposition of A we can split the system into a stable part and an unstable part as in Curtain and Zwart [18, Section 5.2]. Since the unstable part is controllable we conclude that the system is exponentially stabilizable, which implies that it satisfies the finite cost condition. That the system satisfies the dual finite cost condition follows similarly. From the fact that the semigroup is analytic and the control operator not maximally unbounded we conclude that the optimal state feedback is bounded (see Lasiecka and Triggiani [50]). From this it follows that the optimal closed-loop system has an analytic semigroup, a

control operator that is not maximally unbounded and a bounded observation operator. We invoke Curtain and Sasane [9, Theorem 6] to show that the Hankel operator of this closed-loop system is nuclear. This shows that the LQG-characteristic values of the original system are summable (the relation between the Hankel singular values of the closed-loop system and the LQG-characteristic values of the original system are the same as given in Corollary 10.32 for discrete-time systems). □

15.3 Numerical results

For the purpose of numerical investigations we choose the physical parameters in accordance with De Silva [21]. These parameter values are

$$\rho a = 47.2, \quad \alpha = 1.129, \quad \beta = 3.89 \times 10^{-4}.$$

We analyze different approximation techniques using LQG-singular values and Bode diagrams. We only show the Bode diagrams from the first input to the first output, the response from the second input to the second output is similar and the other two responses are zero. Also, we only show the Bode magnitude diagram.

15.3.1 Modal approximation

It is relatively easy to obtain a modal approximation of our model based on the eigenvectors of the fourth derivative operator with boundary conditions as above. For more complicated models of physical systems it will not be easy (or even possible) to obtain a modal approximation. In figure 15.2 the solid line is a Bode-diagram of the 30 dimensional modal approximation. Table 15.1 shows the largest ten LQG-characteristic values for modal approximations.

If we construct the controller mentioned in Remark 14.48 based on a 4 mode approximation it stabilizes the 30 mode approximation, for a design based on a lower order approximation this is no longer the case. Since the unstable subspace is four-dimensional this is of course not very surprising.

15.3.2 Finite-difference approximation

We have obtained finite-difference approximations of our model. In figure 15.2 the dashed line is a 30 dimensional finite-difference approximation and in figure 15.3 the dashed line is a 6 dimensional finite-difference approximation.

Table 15.1: largest 10 LQG-characteristic values for modal approximations

6 modes	10 modes	14 modes	22 modes	30 modes
2.4142	2.4134	2.4134	2.4134	2.4134
2.4135	2.4123	2.4116	2.4111	2.4109
0.4143	0.4146	0.4147	0.4147	0.4148
0.4142	0.4144	0.4144	0.4144	0.4144
0.1071	0.1071	0.1071	0.1071	0.1071
0.1068	0.1068	0.1068	0.1068	0.1068
-	0.1010	0.1010	0.1010	0.1010
-	0.1004	0.1004	0.1004	0.1004
-	0.0009	0.0104	0.0104	0.0104
-	0.0009	0.0102	0.0102	0.0102

From this and the 'intermediate' Bode diagrams not shown it can be seen that the resonance peaks are at too low a frequency and this error converges slowly to zero. The 6 dimensional finite-difference approximation also has an incorrect slope for low frequencies. In table 15.2 the LQG-characteristic values for finite difference approximations are given.

Table 15.2: largest 10 LQG-characteristic values for finite difference approximations

6 dim f-d	10 dim f-d	14 dim f-d	22 dim f-d	30 dim f-d
2.4142	2.4129	2.4129	2.4131	2.4132
0.9964	2.4125	2.4122	2.4116	2.4113
0.9799	0.4146	0.4146	0.4147	0.4147
0.6408	0.4144	0.4145	0.4144	0.4144
0.6394	0.3189	0.2286	0.1711	0.1503
0.4142	0.3183	0.2282	0.1708	0.1500
-	0.1133	0.1255	0.1225	0.1183
-	0.1129	0.1250	0.1219	0.1177
-	0.0089	0.0073	0.0109	0.0114
-	0.0088	0.0072	0.0108	0.0112

We can see here also that the 6 dimensional finite-difference approximation is not good and that convergence is slower then in the modal approximation. However, from the 10 dimensional finite-difference approximation

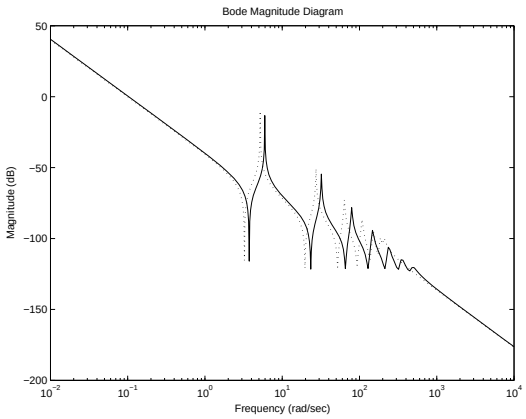

Figure 15.2: 30 mode approximation (-) and 30 dimensional finite difference approximation (:)

on the first four LQG-characteristic values are fairly accurate and the other LQG-characteristic values seem to converge to their correct values. It turns out that the controller mentioned in Remark 14.48 when based on a 6 dimensional finite difference approximation is not stabilizing and that the one based on a 10 dimensional finite difference approximation is. We conclude that controller-design using finite-difference approximations leads to a controller of more than 6 dimensions.

15.3.3 LQG-balanced approximation

We have shown that our model has a compact LQG-balanced realization. Computing this realization exactly is however impossible. The method of LQG-balancing can however be used to obtain good low-order approximations of good high-order approximations. We compute a LQG-balanced realization for the 30 dimensional finite-difference approximation of the beam (this is finite-dimensional LQG-balancing, so it can be done using an algorithm from finite-dimensional theory). The Bode diagram of a 14 dimensional LQG-balanced truncation of the 30 dimensional finite-difference approximation of the beam is shown in figure 15.4 and that of a 4 dimensional LQG-balanced truncation of the 30 dimensional finite-difference approximation of the beam is shown in figure 15.5.

As can be seen the approximation is about as good as can be expected given the order of the approximation. The controller mentioned in Remark 14.48 when based on a 4 dimensional LQG-balanced truncation of a 30 dimensional finite difference approximation stabilizes the 30 dimensional modal approximation. Thus it can be expected that it will stabilize the beam.

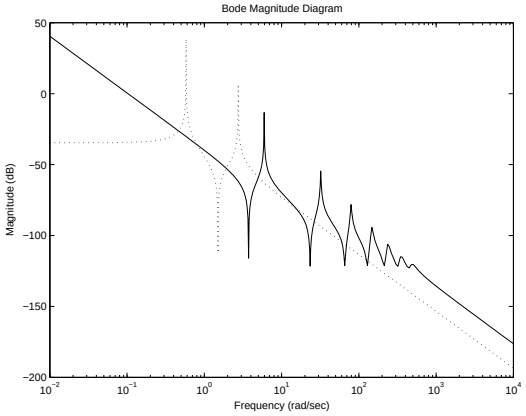

Figure 15.3: 30 mode approximation (-) and 6 dimensional finite difference approximation (:)

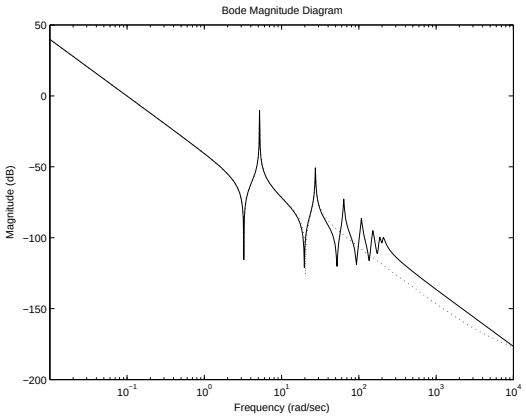

Figure 15.4: 30 dimensional finite difference approximation (-) and its 14 dimensional LQG-balanced truncation

15.4 Conclusion

We showed that a finite difference approximation followed by a LQG-balanced truncation gives a stabilizing 4 dimensional controller. This is as good as can be obtained using a modal approximation. A stabilizing controller based only on a finite difference approximation must have more then 6 states. This shows that the combination of a finite difference approximation and LQG-balancing is better than a finite difference approximation alone.

We note that it is crucial for the analysis presented here that the damping parameter β is positive. If $\beta = 0$, then one can show that the LQG-characteristic values do not form a summable sequence. Controllers designed

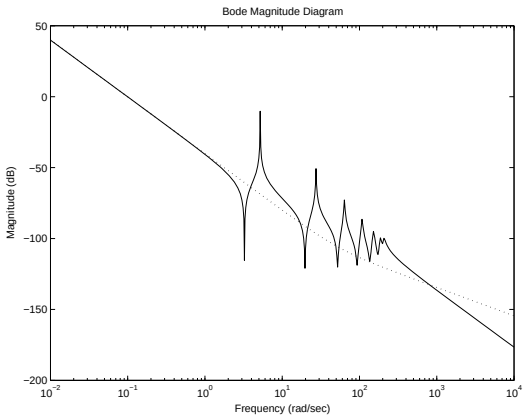

Figure 15.5: 30 dimensional finite difference approximation (-) and its 4 dimensional LQG-balanced truncation (:)

based on approximations in this case do not give a satisfactory performance in numerical simulations.

Notes

The beam model presented here was thoroughly analyzed in Bontsema [6]. Proposition 15.1 and the numerical results presented here were reported earlier in Opmeer, Wubs and Van Mourik [73]. The numerical results are based on Van Mourik [92], where many more numerical results concerning our example can be found. Some more numerical work on LQG-balanced realizations can be found in Evans [24].